PCCP

Accepted Manuscript

ROYAL SOCIETY OF CHEMISTRY

www.rsc.org/pccp

Infrared study of matrix-isolated ethyl cyanide : simulation of the photochemistry in the atmosphere of Titan

A. Toumi*, N. Piétri, I. Couturier-Tamburelli*

Aix-Marseille Université, CNRS, PIIM, UMR 7345, 13397 Marseille, France

Abstract

Low-temperature Ar matrix isolation has been carried out to investigate the infrared spectrum of ethyl cyanide (CH_3CH_2CN), molecule present in the atmosphere of Titan. The λ>120 nm and λ>230 nm photolysis in Ar matrix of ethyl cyanide were also performed in order to compare the behaviour of this last compound when it is submitted to high and low energetic radiations. These different wavelength have been used with the aim to reproduce the radiation reaching the various parts of the atmosphere. Several photoproducts were identified during photolysis such as vinyl cyanide (CH_2=CHCN), cyanoacetylene (HC_3N), ethylene/hydrogen cyanide (C_2H_4/HCN), ethylene/hydrogen isocyanide (C_2H_4/HNC), acetylene/hydrogen cyanide (C_2H_2/HCN), acetylene/hydrogen isocyanide (C_2H_2/HNC), and acetylene:methylenimine (C_2H_2:$HNCH_2$) complexes. Ethyl isocyanide (CH_3CH_2NC) and a ketenimine form (CH_3CH=C=NH) have been identified as well. Photoproducts identification and spectral assignments were done using previous studies and density functional theory (DFT) calculations with the B3LYP/cc-pVTZ basis set.

Corresponding authors: isabelle.couturier@univ-amu.fr, abdelkrim.toumi@univ-amu.fr,

Introduction

Titan, the biggest Saturn's satellite, was discovered in 1655 by the Dutch astronomer Christian Huygens. It is an unique case in the Solar System because it is the only satellite with a dense atmosphere composed of two major constituents: nitrogen (N_2) [1,2] and methane (CH_4).[3] A photochemistry of these main components occurs at high altitude in the atmosphere by solar photons, cosmic rays and a heavy bombardment of electrons from Saturn's magnetosphere.[4] Since then, Titan became more and more interesting as numerous species were identified in its active atmosphere thanks to detections performed from Earth or during different spatial programs (Voyager I and II, Cassini-Huygens). Most of them are hydrocarbon and nitrile species like diacetylene (C_4H_2), dicyanoacetylene (C_4N_2), cyanoacetylene (HC_3N).[5,6] The Cassini orbiter and the Huygens probe performed *in situ* analysis which permitted the identification of $CH_3CH_2CNH^+$[7] present in gas phase and a recent study confirms the detection of ethyl cyanide (CH_3CH_2CN) in the atmosphere of Titan via its emission lines[8] thanks to the Atacama Large Millimeter/submillimeter Array (ALMA). The identification of solid phase ethyl cyanide in Titan was suggested by Khanna[9] and the molecule was also detected in the dense molecular clouds Sagittarius B_2 and OMC-1 (in the Orion's nebula).[10]

Its gas phase formation has been envisaged by Krasnopolsky[11] using the work of Herron[12], showing that ethyl cyanide can be formed by recombination processes including both electronically excited states of nitrogen, see reactions (1) and (2), in which kinetic reaction rates have been determined at room temperature. These reactions can occur in the atmosphere of Titan (reactants obtained from the photolysis of N_2 and the presence of C_3H_6) such as they were included in recent models for the atmospheric photochemistry in Titan[11].

(1) $N^*(^2D) + C_3H_6 = C_2H_5CN + H^*$; k_1 (298 K) = 6.6×10^{-11} cm^3 molecule^{-1} s^{-1}

(2) $N^*(^2P) + C_3H_6 = C_2H_5CN + H^*$; k_2 (298 K) = 1.9×10^{-12} cm^3 molecule^{-1} s^{-1}

Spectroscopic investigations of ethyl cyanide (Cs symmetry) have been published in liquid and vapor phases with infrared[13,14,15,16,17], Raman[13,14,15] and microwave[18,19,20,21,22,23,24,25,26,27] techniques. Solid phase infrared spectra have been carried out by Dello Russo and Khanna[28]and Khanna.[9] No detailed infrared analysis of ethyl cyanide in cryogenic matrix has been found in the literature.

The VUV spectroscopy was first studied by Cutler[29] in the 100-180 nm region. Only a small absorption band was pointed out at 134.2 nm and might be corresponding to the C-C absorption. Using electron impact spectroscopy to study ethyl cyanide, Stradling and Loudon[30] found a first structure at 193.7 nm that could be due to triplet excitation and three Rydberg transitions series converging to the first ionization potential (101.5 nm) in the 91-208 nm region. Lake and Thompson[31] determined the vertical ionization potential from the CN π group at 102.5 nm (95468 cm^{-1}). The 0-0 transition is at 104.7 nm with a progression interval of about 2100 cm^{-1}. Later, Kanda et al.[32] calculated the first ionization potential to be 108.0 nm and found more transitions between 99 and 134 nm.

Hudson and Moore[33] studied the photochemistry of CH_3CN and molecules with sequential substitution of each H atom by a methyl group (CH_3) such as CH_3CH_2CN (ethyl cyanide), $(CH_3)_2CHCN$ and $(CH_3)_3CCN$. This study was performed in solid phase and in N_2 or H_2O matrices induced by proton bombardment and VUV irradiation. In the case of ethyl cyanide, they observed the formation of hydrogen cyanide (HCN) and ethyl isocyanide (CH_3CH_2NC). A ketenimine form ($CH_3CH=C=NH$) and vinyl cyanide ($CH_2=CHCN$) were also identified.

In this work, we report a detailed infrared analysis of ethyl cyanide when it is trapped in Ar matrix. We also present the results about the photolysis of Ar matrix-isolated ethyl cyanide with an hydrogen-flow lamp (λ>120 nm) and a mercury lamp (λ>230 nm) in order to simulate the different energies for photodissociation processes available at high and low altitude in the atmosphere of Titan. The identification of the photoproducts obtained is performed using previous experiments and calculation.

Experimental section

Ethyl cyanide (hereafter **1**) is available commercially (from Aldrich, 99%) and was degassed several times with nitrogen and nitrogen-ethanol baths in order to avoid the presence of impurities. The experimental technique and the apparatus were already described earlier.[34] The matrix was obtained by mixing **1** with argon (Ar) or nitrogen (N_2) in a pyrex line and then deposited onto a golden copper plate cooled at 20 K thanks to a 21 CTI cold head model. The dilution ratios (**1**/gas) were approximately 2/500 and were determined by standard manometric techniques. Spectra were recorded at 20 K using a Fourier transform infrared spectrometer (Nicolet serie II Magna System 750) in the 4000-650 cm^{-1} region with a MCT detector in reflection-absorption mode. Each spectrum was averaged over 100 scans with a

0.125 cm^{-1} resolution. The UV-Visible spectrometer is a Lambda 20 Perkin-Elmer. The spectrum was acquired between 300 and 700 nm (**1** was introduced in a quartz cell) with a 1 nm resolution.

High energetic photolysis experiments were carried out with a microwave discharge hydrogen flow lamp (Opthos Instrument, λ>120 nm) through a MgF_2 window connected to the cryostat. The total flux of this last lamp has been calculated earlier with the actinometric method to be 4.79 (±1.37) × 10^{13} photons cm^{-2} s^{-1}.[35] Photolysis experiments have also been performed using an Osram 200 W high-pressure mercury lamp equipped with a quartz envelope (λ>230 nm) with an estimated flux of about 2.75 × 10^{16} photons cm^{-2} s^{-1}.[36,37]

Density functional theory (DFT)[38,39,40] was used to calculate the vibrational spectra of the reactants and the reaction products. The Gaussian 09[41] program package using the B3LYP[42,43] procedure with a cc-pVTZ basis set was used for these calculations. TD-DFT calculations was used to simulate UV spectra and to determine the molecular orbitals (MO) involved in each transition.[43,44]

Results

1. Infrared spectroscopy of ethyl cyanide 1 in Ar matrix

17 (on 21) of the fundamental modes of vibration of **1** (Cs symmetry) are located in the 4000-650 cm^{-1} region and some harmonic and combination modes are also observed. A' and A" symmetry fundamental modes are assigned from ν_1 to ν_{13} and from ν_{14} to ν_{21} respectively. Figure 1 shows different regions of the infrared spectrum of **1** trapped in Ar matrix (2/500) and all the values concerning the infrared absorption bands (wavenumber and relative intensities) are listed in Table 1 and compared with the work of Klaboe and Grundnes[14] which is the most detailed previous analysis and those of Wurrey et al.[15]0 In the matrix-isolated spectrum, a few bands can correspond to one vibrational mode which is characteristic of different trapping sites of the molecule within the matrix.

We performed calculation in order to determine the theoretical infrared spectrum in gas phase of **1** and compared the results obtained with our experiment in matrix and other previous experiments performed in gas phase.[13,14,15]

The most intense bands of the infrared spectrum of **1** in Ar matrix are located in the area of the ν_{CH} stretching modes. For the band at 3006 cm^{-1} a shoulder is located at 3001 cm^{-1}. Numerous authors[13,14,15,16,17] attribute theses bands to both ν_1 and ν_{14} in gas phase. According

to our calculation, in which the ν_{14} and ν_1 modes are predicted to be separated by only 4 cm^{-1}, we attribute respectively to ν_{14} and ν_1 modes the bands observed at 3006 and 3001 cm^{-1}, the most intense of the whole infrared spectrum being the ν_{14} mode. In the same area, another band (2961 cm^{-1}) is very intense and it corresponds to the ν_2 mode.

The two other most intense bands are located at 1467 and 1460 cm^{-1} and correspond to the symmetric stretching CH (ν_5) and asymmetric CH (ν_{16}) deformations. These two modes (ν_5 and ν_{16}) are predicted by our calculation at 1462 and 1454 cm^{-1} respectively. These modes are observed at 1476 (1466) and 1462 (1457) by Wurrey et al.[15] in gas phase (solid phase) .Two other bands lightly less intense are also observed at 2255 and 1075 cm^{-1}. According to the previous gas phase study[15], they are attributed to the ν_4 CN stretching (2255 cm^{-1}) and to the ν_9 modes (1075 cm^{-1}). Nevertheless a difference is observed with this work concerning the ν_{18} mode. Indeed, this mode is observed respectively at 918 and 1000 cm^{-1} by Klaboe and Grundnes[14] and Wurrey at al. [15]. In our work, we don't observe absorption bands in this area. Nevertheless, a band at 1095 cm^{-1} is observed. So we attributed this band to the ν_{18} calculated at 1084 cm^{-1}. With our assignment (ν_{18} at 1095 cm^{-1} and ν_9 at 1075 cm^{-1}), we respect the calculated separation between the two modes (21 cm^{-1}).

Trapping **1** in Ar matrix permits to observe many harmonic and combination bands as mentioned in Table 1. By following the assignments made by Klaboe and Grundnes[14],we noticed some differences. Based on the solid phase experiment, the band observed at 2895 cm^{-1} is attributed to the $2\nu_{16}$. The small band located at 2787 cm^{-1} is assigned to $\nu_{12}+\nu_4$ combination mode by comparison with the raman spectrum in liquid phase. On the other side, those observed at 2300 cm^{-1} in argon matrix corresponds to the band observed at 2297 cm^{-1} in liquid raman and we attributed it to the $\nu_{10}+\nu_8$ combination mode counter to Klaboe and Grundnes[14].

2. C_2H_4:HCN complex (**C1**) in argon matrix

2.1. Infrared characterization of **C1** in argon matrix

Based on our previous work concerning the photochemistry of vinyl cyanide[45] in which C_2H_2:HCN and C_2H_2:HNC complexes (noted **C2** and **C'2** respectively, see Scheme 1) have been obtained after photolysis and on the literature data, we expected the formation of C_2H_4:HCN and C_2H_4:HNC complexes (noted **C1** and **C'1** respectively) from the photochemistry of ethylcyanide. So we decided to perform an infrared study of a

C_2H_4/HCN/Ar mixture in order to determine the spectral assignment of **C_1** and **C'_1** and to see if they are produced during the photolysis experiment of **1** as expected.

A C_2H_4/HCN/Ar mixture (1/5/1000) was deposited at 20 K and then irradiated with the hydrogen flow lamp (λ>120 nm). The deposition permitted us to define the bands belonging to **C_1** by comparing with the spectra of monomers at the same temperature as shown in Figure 2 and by comparing also their evolution when irradiation occurs. The bands noted with **C_1** are assigned to one complex form (with a correlated evolution). We noticed the presence of a band at 3188 cm^{-1} that has not an evolution similar to the other ones and this band remains unassigned.

Similarly to our previous work[45] and to previous work concerning complexes involving ketene with HCN or HNC and the work of Kukolich et al.[46], we envisaged two plausible geometries for **C_1** (Figure 3): the first one, called π-form, where the hydrogen atom of HCN is in interaction with the double bond of C_2H_4 and a second one, a planar form (called ρ-form), with an interaction between the nitrogen atom of HCN and one hydrogen of C_2H_4. After the BSSE correction, the π-form is more stable in energy by 7.1 kJ mol^{-1} than the ρ-form and it is stabilized by 1.75 kJ mol^{-1} compared to monomers. The calculated and experimental wavenumbers of both forms (π- and ρ-form) of **C_1** are noted in Table 2. The ρ-form implies lesser shifts for the HCN fundamental vibration modes than the π-form. The CH stretching mode of HCN is predicted to be shifted toward lower frequencies by 62 cm^{-1} for the π-form and by 5 cm^{-1} for the ρ-form while the observed experimental shifts are 60 cm^{-1}. The degenerated deformation mode of HCN is shifted to higher frequencies by 39 and 35 cm^{-1}. The calculated shifts of the π-form are 48 and 44 cm^{-1} while the shifts are almost none for the ρ-form. The comparison between experimental and theoretical wavenumbers allows us to conclude that the π-form is generated (Table 2). Our result are in agreement with those of Kukolich et al.[46b] They obtained a "T-shaped" complex in which the HCN molecule is perperdicular to the ethylene's plane with a HCN carbon atom located at 3.702 Å above the ethylene plan (3.707 Å in our calculations).

2.2. Irradiation of C_1 in Ar matrix

We have to take into account the fact that we are in presence of C_2H_4 and HCN monomers and will be also irradiated. When we submitted **C_1** to high energetic irradiation (λ>120 nm), a decrease in intensity of the complex bands is observed and new absorption bands grew up (Figure 4). Some of them are also observed during the irradiation of HCN/Ar

and C_2H_4/Ar and we are not interested with these last ones. Among the products formed are found C_2H_2:HCN, noted **C_2** (3281, 3234, 2094 and 753 cm^{-1}) and C_2H_2:HNC, noted **C'_2** (3441, 3276, 2031 and 751 cm^{-1}) complexes (Scheme 2), based on our previous study[45] where we showed that the two complexes are formed by irradiating vinyl cyanide (**3**). Their geometries are known to be analogous to the case of **C_1**: the hydrogen atom of HCN (or HNC) is in interaction with the triple bond of C_2H_2. The presence of bands located at 3315, 2269, 2076 and 667 cm^{-1} shows that the formation of cyanoacetylene (HC_3N, **5**) has been obtained by irradiating **C_1** and the produced **C_2**. Since **5** is well known to induce izomerisation process under UV irradiation, we have considered the formation of some of them. Thus we have identified the formation of isocyanoacetylene HC_2NC (3328, 2213 and 2033 cm^{-1}), $HCNC_2$ (3276, 2102 and 1920 cm^{-1}) and the carbene imine (3562, 2204 and 1906 cm^{-1}).[46]

Two bands observed at 3449 and 2028 cm^{-1} have the same evolution during the experiment. Since the complex C_2H_2:HNC is formed during the photolysis, we attributed the band at 3449 cm^{-1} to ν_{NH} and the one at 2028 cm^{-1} to ν_{NC} when the HNC is complexed to C_2H_4 (**C_1'**). These adsorption bands are shifted by -171 and -1 cm^{-1} to lower frequencies with respect to ν_{NH} and ν_{NC} modes of HNC monomer respectively (Table 2). For the ν_{NH} of **C_1'** the theoretical shifts are predicted to be -165 and -1 cm^{-1} for the π and ρ complex respectively, while it is -171 cm^{-1} experimentally. Therefore, we can assume that these frequency shifts are due to the formation of a complex noted **C_1'** between C_2H_4 and HNC with a π form trapped in the same cage during the photolysis of **C_1**. (Scheme 1). At last, three bands located at 3298, 3260 and 1968 cm^{-1} (Figure 4) appeared during the irradiation, but they are too small to be properly integrated in order to perform a correlation. Nevertheless the vicinity of the bands with the C_2H_2:HCN/HNC (**C_2**, **C_2'**) complexes led us to suppose the formation of a new complex involving C_2H_2.

3. Irradiation (λ>120nm and λ>230nm) of ethyl cyanide

When we submitted **1** to VUV irradiation during 1267 minutes with the help of a hydrogen-flow lamp (λ>120 nm) in Ar matrix, we observed a decrease in intensity for the bands attributed to **1** and noticed the appearance of new absorption bands (Figure 5). By checking the evolution of their integrated absorbance during the irradiation, we are able to group them in sets of bands (the bands belonging to the same photoproducts will evolve the same way).

All the structures of the products formed during the photochemical experiment are summarized in Scheme1.

Isonitrile are well-known products in nitriles' photolysis and the NC stretching mode region is located between 2100 and 2200 cm^{-1} approximately. Based on our previous work concerning the photochemistry of acrylonitrile[45], we attributed the band located at 2151 cm^{-1} to ethyl isocyanide. A weak band at 2152 cm^{-1} with the same evolution during the irradiation is found. The vicinity of these two bands leds us to suggest that there are two trapping sites in the matrix (rather than two different modes belonging to the same product). During their work, Hudson and Moore[33] identified ethyl isocyanide, CH_3CH_2NC (hereafter **2**), as a product of **1** when photolyzed in solid phase with a band at 2160 cm^{-1}. Bolton et al.[47] published rotation and infrared spectra of **2** and the νNC stretching mode is located at 2148 cm^{-1} (liquid phase) and 2155 cm^{-1} (vapour) and is found to be the most intense in the infrared spectrum of **2**. Calculation predicted the NC stretching mode of **2** to be located at 2147 cm^{-1}. We are able to conclude that the isonitrile **2** was photoproduced by the irradiation of **1** even if no other band of **2** was observed.

In an earlier work[45], we studied the photolysis of vinyl cyanide, CH_2=CHCN (hereafter **3**) in Ar matrix. The most intense modes of **3** and specially those at 974 and 953 cm^{-1} are observed in Ar matrix. We noticed that two bands appeared at 972 and 955 cm^{-1} during the irradiation of **1** and are attributed to **3**. A small difference in wavenumber is usual when we compare infrared spectra of matrix-isolated and photoproduced product within a matrix.[48] Another band, located at 881 cm^{-1}, could be attributed to **3** but this last band is too weak to be properly integrated. Since **3** is a known product of the photolysis of **1**, the photoproducts of **3** are suspected to be formed during our experiment. Based on our previous work and on the results obtained in the 2.2 section, we identified cyanoacetylene (HC_3N) noted **5** [49,50] and three of its isomers: HNC_3[49,51,52], HC_2NC[49,53] and $HCNC_2$[49,53]. The products obtained from the photochemistry of **5** are noted **5'**. The photolysis of **3** also gives the generation of vinyl isocyanide (CH_2=C(H)NC, noted **4**) and a set of bands located at 2125, 1629, 1116 and 921 cm^{-1} agrees with the formation of **4** from the photolysis of **1**.

In their study about solid phase photolysis of **1**, Hudson and Moore[33] demonstrated the formation of a ketenimine form (CH_3CH=C=NH, noted **6**). The formation of **6** is accompanied by the growth of a band at 2032 cm^{-1} in the parent nitrile in solid phase. This product is also formed in N_2 and H_2O matrices by both proton bombardment and UV photolysis. In our case, a band (not yet assigned) grew at 2043 cm^{-1} (along with a weaker one at 2037 cm^{-1}) during the photolysis in Ar matrix. This value is still in agreement with the one

obtained by Hudson and Moore (shift observed between matrix-isolated and solid phase) and with the calculation (see Table 3). But, another band located at 857 cm^{-1}, not found by Hudson and Moore, grew with a similar evolution with the band at 2043 cm^{-1}. One fundamental mode is predicted by the theory to be located at 851 cm^{-1} in gas phase (Table 3). So, we can conclude that **6** is photoproduced by irradiating **1** and the band at 857 cm^{-1} belongs to **6**.

We observe four bands located at 3243, 2093, 1441, and 958 cm^{-1} which are very close to those obtained during the $\mathbf{C_1}$ trapped in Ar matrix experiment (previous part (**2.1.**)). These very small shifts are indicative of the $\mathbf{C_1}$ formation (Table 2). The formation of $\mathbf{C'_1}$ is also observed and the bands are located at 3467, 2026 and 967cm^{-1}. It is of interest to compare present $\mathbf{C_1'}$ spectrum with those obtained during vacuum-UV irradiated $\mathbf{C_1}$ complex in Ar matrix (Table 2). Small spectral shifts, usually different for the two types of precursors (bimolecular and propionitrile), are observed. These are due to the specificity of Ar matrix cages inhabited by photochemically generated species $\mathbf{C_1'}$ from **1**, with other possible reaction products (in particular H_2) remaining in their close vicinity. A good agreement is found between experimental and theoretical shifts between complexes and monomers. $\mathbf{C_2}$ and $\mathbf{C'_2}$ complexes were also formed as for the irradiation of $\mathbf{C_1}$.

At last the five bands (3298, 3260, 1969, 1068 and 740 cm^{-1}) previously observed in very small amounts during the photolysis of $\mathbf{C_1}$ have the same evolution during the photolysis experiment of **1** (Figure 6). Taking into account the proximity of these bands with those of the C_2H_2/HCN or HNC complexes, we have considered the formation of a new complex. Since the UV irradiation of **1** can induce the formation of C_2H_2 trapped with HCN/HNC and H_2 we have supposed that the irradiation of **1** can led to the generation of C_2H_2 with $HNCH_2$ noted $\mathbf{C_3}$ (Scheme 1). In order to model the complex structure and its vibrational spectrum, theoretical calculations were performed on different starting geometries. Only one energy structure minimum is obtained. The optimized structure is shown in Figure 3. This complex exhibits two hydrogen bonds between the acetylene C≡C triple bond and two of the hydrogens of the methylenimine (2.89 and 3.41 Å respectively). This complex is not planar, the two partners are located in perpendicular planes. After BSSE correction this complex is stabilized with regard to the monomer molecules by 3.45 kJ/mol. The calculated frequencies of this complex and the monomers are summarized in Table 4. The comparison between experimental and theoretical frequencies allows us to conclude on the $\mathbf{C_3}$ formation during the **1** photochemistry. The bands observed at 3260 and 1969 cm^{-1} are shifted to lower frequencies by 3 and 5 cm^{-1} respectively, while 2 and 3 cm^{-1} are predicted by the calculation.

Nevertheless, the band located at 3298 cm^{-1} is shifted experimentally to higher frequencies through it is predicted to be red shifted by the calculation. This fact is well known since the photochemically generated complex exhibits frequencies lightly different from those of the deposited complex.

The photolysis of **1** in Ar matrix with a less energetic irradiation source (mercury lamp, λ>230 nm) has been investigated. An UV-Visible spectrum of **1** was recorded with our means between 200 and 800 nm showing very weak absorptions at 325, 520 and 630 nm. After 1620 minutes of photolysis, we didn't observe any decrease of **1** absorption bands but only the appearance of very weak bands belonging to impurities.

UV calculation

Since no UV data have been found concerning **2**, TD-DFT calculations were used to simulate the UV spectrum and to determine the MO's involved in each transition. These calculation were performed in argon with B3LYP method. The calculated UV spectral data are given in Figure 7 for **1** and **2**.

The theoretical UV spectrum of **1** has been calculated in order to verify that it is in agreement with the experimental data. We observed on the theoretical spectrum all the absorption previously obtained with experiments[29,30,31,32].

The theoretical UV spectrum of **2** presents two intense absorptions. The most intense vertical TD-DFT B3LYP/6-31g** calculation predicts a band at λ=122 nm, with allowed electronic transition from S_0 with a high oscillator strength (f= 0.3557). In this transition four single-electron transitions contribute. The molecular orbitals responsible for these transitions are shown in Figure 8. As it appears in this figure, the single electron transitions from molecular orbitals 12 and 13 move electron density from CH_3 fragment onto isonitrile substituent. The second one is predicted at 151 nm and corresponds to two different transitions from S_0 to S_2 and S_5 which have oscillator strengths very close (f=0.0570 and 0.0580 respectively). The main molecular orbitals responsible for these transitions are 15 to 16 (with a small contribution of 13 to 16 and 14 to 17) and 15 to 17. For the 15 to 17 transition, the electron density moves in the opposite direction from the σ planar. As a consequence, since **2** absorbs at λ>120 nm it is not surprising to observe an equilibrium between the formation and the destruction of **2**.

4. Discussion

Here, we demonstrate the formation of the isonitrile **2** and this work corresponds to the first identification of this compound in Ar matrix. The C-C bond dissociation energy of CH_3CH_2-CN has been calculated to be 32870 cm^{-1} or 304.2 nm.[54] So, the irradiation with λ>120 nm and λ>230 nm could permit the C-CN cleavage and a rotation of the CN terminal group to give **2** as observed in numerous studies concerning nitriles photochemistry.[45,46,49] The evolution of the integrated absorbance of the band at 2151 cm^{-1} (Figure 9) concerning **2** evolves as an intermediate species. By means of photoelectron spectroscopy, Wang and Qian[55] studied the isomerization reaction of **2** turning into **1**. They showed that **2** is a quiet stable compound at room temperature and determined isomerization rates at different temperatures leading to an activation energy (E_a) of 38.36 (±0.32) kcal mol^{-1} which is in good agreement with previous results.[56] This E_a value indicates that at λ≤745 nm this reaction is possible. So, the isomerization of **2** to **1** can be easily considered in our cases (λ>120 nm) since **2** absorbs in this range of wavelength (predicted bands at 122 and 151 nm (Figure 7)).

During the first part of **1** photolysis, the photochemical reaction leading to **2** is much more efficient than the reverse reaction (from **2** to **1**). The ethyl isocyanide starts to decrease after 300 min of irradiation (Figure 9). In the second part, there is a competition between production and consumption of **2**. We supposed the photogeneration of a lot of compounds (Scheme 1). **3**, **4**, **C$_2$** and **C'$_2$** from **2**. Vinyl cyanide **3** and vinyl isocyanide **4** have been identified. The evolution of **3** and **4** bands versus time (Figure 9) shows that these two compounds are formed faster than they are destroyed. **3** is formed by dehydrogenation of **1**. This reaction is well-known and is applied industrially.[57] Based on our previous work[45], when **3** is produced, it undergoes photodissociation processes and gives **4** with a similar process than for the formation of **2** from **1**. We can also suppose the formation of **4** from dehydrogenation of **2**. Other photoproducts of **3** were found: **5** (HC_3N), **C$_2$** (C_2H_2:HCN), **C'$_2$** (C_2H_2:HNC) complexes.

In this work, we were interested with complexes implying C_2H_4 and HCN/HNC (**C$_1$** and **C'$_1$**) in cryogenic matrices. We succeeded in identifying the geometry and the infrared spectrum of **C$_1$**. The irradiation of **C$_1$** trapped in Ar matrix lead to the formation of **C'$_1$** (i.e.

from HCN to HNC), identified as a photoproduct of **1** using calculation. Its formation can be due to the irradiation of **2** or $\mathbf{C_1}$.

When trapped in cryogenic matrix, **1** is surrounded by rare gas. This permits intramolecular rearrangement and we identified the ketenimine form **6** resulting from the CH (of the $-CH_2-$ group) breaking and a 1,3-migration toward the CN terminal group. The ketenimine grows during the first 300 min (Figure 9), thereafter it remains constant showing that this compound is formed as fast as it is destroyed.

At last, $\mathbf{C_3}$ obtained in very small quantity during the $\mathbf{C_1}$ irradiation is formed in bigger amount during the **1** photolysis. This is coherent with the fact that the $\mathbf{C_1'}$ complex is obtained in bigger amount during the **1** photochemistry. With this consideration we can suppose that $\mathbf{C_3}$ is obtained from the $\mathbf{C_1'}$ irradiation

$$C_2H_4{:}HCN\ (\mathbf{C_1}) \rightleftharpoons C_2H_4{:}HNC\ (\mathbf{C_{1'}}) \longrightarrow C_2H_2{:}HN{=}CH_2(\mathbf{C_3})$$

This methylenimine complex $\mathbf{C_3}$ rose continuously during all of the photolysis experiments (Figure 9) showing that this compounds is formed faster than it is destroyed. CH_2NH is an important molecule since its presence has been suggested in Titan's upper atmosphere.[7]

Using an hydrogen-flow lamp (λ>120 nm), we simulated the solar flux arriving in the atmosphere of Titan at high altitude. **1** is present in traces form and is submitted to this irradiation (along with cosmic rays and a heavy bombardment from Saturn's magnetosphere). Each molecule present in gas phase in the atmosphere of Titan is more surrounded by N_2 than by other molecules due to the N_2 abundance. The cryogenic matrix isolation method is used in order to see the becoming of each isolated molecule. Compared to the gas phase, it seems clear that we cannot have the formation of the four complexes which is clearly a consequence of the cryogenic matrix trapping. The formation of the ketenimine form **6** is neither envisaged in gas phase because of the high volability of the H radical when it is produced (rather than an intramolecular rearrangement) but this specie has been previously obtained in solid phase. Titan is known to possess a characteristic halo of hydrogen at high altitude composed by hydrogen liberated mainly from atmospheric CH_4.[58] We have also to take into account that the temperature present in high altitude (>500 km) of the atmosphere is higher than 140 K[59], which is not compatible with a cryogenic matrix experiment.

Other photoproducts of **1** have already been identified in the atmosphere of Titan such as vinyl cyanide (**3**)[60], cyanoacetylene (**5**)[61], hydrogen cyanide (HCN)[62], ethylene (C_2H_4)[62] and hydrogen isocyanide (HNC).[63] The photoproduction from **1** of these compounds in the atmosphere is highly envisaged. The isonitrile compounds formed (except HNC) may be not

present in enough quantity to be observed and this can explain the difficulties to detect them in the atmosphere of Titan.

By using the mercury lamp (λ>230 nm), we simulate the processes occurring at low altitude in the atmosphere of Titan. The abundance of **1** in the atmosphere is probably too low to measure its vertical distribution yet. In the case of its presence in the troposphere of Titan (altitude lower than 50 km), **1** can be submitted to longer wavelengths but with no occurring photochemistry. **1** is stable upon this kind of irradiation and long-lived at low altitude.

5. Conclusion

Ethyl cyanide is a known component of the atmosphere of Titan. A detailed infrared analysis of ethyl cyanide has been performed. Trapping in cryogenic matrices of Ar permitted to obtain thinner absorption bands and avoided, for the first time, any ambiguity in the assignment resulting from different previous results with infrared spectroscopy[13,14,15,16,17] concerning both vapor and liquid phases.

The photodissociation (λ>120 and >230 nm) of ethyl cyanide has been investigated in order to see the behavior of such a molecule in gas phase at high and low altitude in Titan's atmosphere. Concerning ethyl cyanide, its behavior changes with the range of wavelength implied in the irradiation. This study revealed the formation of vinyl cyanide and a lot of products are resulting from its photolysis. Compared to our previous study[45], we characterized a new complex implying C_2H_4 with HCN/HNC. This characterization was made with help of a C_2H_4/HCN/Ar photolysis experiment.

6. Aknowledgements

Authors express their gratitude to Dr. A. Allouche (CNRS, UMR 7345) for the valuable discussion concerning the calculation.

Figures and tables

Assignment	Wavenumber (cm^{-1})			
	solid[b]	Gaseous phase[a,b]	Ar matrix (rel. Intensity)	Theory B3LYP/cc-pVTZ (sym./ rel. intensity)
$\nu_8 + \nu_4$		3571[a]	3573 (1)	-
$\nu_{13} + \nu_2$		3259[a]	3259 (2)	-
$\nu_{13} + \nu_3$		3204[a]	3216 (1)	-
$\nu_{11} + \nu_4$		3098[a]	3087 (2)	-
ν_{14}	2997	3006[a]	3006 (100)	3027 (A" / 90)
ν_1		3005[b]	3001 (27)	3022 (A' / 94)
ν_{15}	2973		-	2980 (A" / 6)
ν_2	2955	2963[b]	2961 (42)	2956 (A' / 100)
ν_3	*2941*	*2950*[b]	2943 (8)	2951 (A' / 24)
$\nu_5 + \nu_6$		*2910*[b]	2903(5)	
$2\,\nu_{16}$	2897		2895 (15)	
$2\nu_6$		2858[a]	2850 (<1)	-
$\nu_{12} + \nu_4$	***2790***[a]		2787 (<1)	-
$2\nu_7$		2757[a]	2754 (2)	-
$2\nu_8$		2636[a]	2628 (2)	-
$\nu_9 + \nu_5$		2520[a]	2523 (<1)	-
$\nu_9 + \nu_7$		2462[a]	2457 (<1)	-
$\nu_9 + \nu_8$		2395[a]	2390 (<1)	-
$\nu_{10} + \nu_8$	***2297***[a]		2300 (<1)	-
$\nu_{11} + \nu_6$		2269[a]	2270 (<1)	-
ν_4	2244	2261[a,b]	2255 (22)	2282 (A' / 50)
$\nu_{11} + \nu_7$		2219[a]	2211 (1)	-
$\nu_{19} + \nu_7$		2040[a]	2043 (<1)	-
ν_5	1466	1476[b]	1467 (38)	1462 (A' / 30)
ν_{16}	1457	1462[b]	1460 (37)	1454 (A" / 37)
ν_6	1430	1442[b]	1437 (17)	1432 (A' / 27)
ν_7	1381	1394[b]	1387 (12)	1378 (A' / 6)
ν_8	1323	1323[b]	1321 (6)	1311 (A' / 16)
ν_{17}	1268	1267[b]	1263 (<1)	1253 (A" / 0)
$\nu_{20} + \nu_{19}$		1164[a]	1161 (<1)	-
ν_{18}		918[a] ; 1000[b]	1095 (6)	1084 (A" / 2)
ν_9	1077	1074[a]	1075 (31)	1062 (A' / 18)
ν_{10}	1014	1008[a]	1006 (3)	982 (A' / 2)
ν_{11}	835	835[b]	834 (<1)	814 (A' / 1)
ν_{19}	778	783[a]	782 (34)	768 (A" / 18)
$2\nu_{20}$		731[a]	737 (1)	-

Table 1: Experimental and theoretical (B3LYP/cc-pVTZ, scaled with a 0.96 factor) wavenumbers of **1**. (a) = ref 14 ; (b) = ref 15.
Values in italic are obtained from Raman spectrum. Values in bold are obtained from liquid spectrum

	Experimental				Calculation (B3LYP/cc-pVTZ)				
	Monomer	Deposited	Photoproduced from **1**	$\Delta\nu_{dep}$ ($\Delta\nu$**1**)	Monomer	π	ρ	$\Delta\nu_{\pi}$	$\Delta\nu_{\rho}$
C_2H_4	3111	-	-	**-**	3095	3096	3094	**1**	-1
	2995	2997	-	**2 (-)**	3001	3002	2999	**1**	-2
	1440	1442	1441	**2 (1)**	1420	1422	1424	**2**	4
	947	961	958	**14 (11)**	940	954	937	**14**	-3
HCN	3303	3243/3232	3243	**-60/-71 (-60)**	3313	3251	3308	**-62**	-5
	2098	2092	2093	**-6 (-5)**	2113	2107	2116	**-6**	3
	721	760	-	**39 (-)**	732	780	732	**48**	0
	721	756	-	**35 (-)**	732	776	731	**44**	-1
		Photoproduced from **C**$_1$		$\Delta\nu$**C**$_1$ ($\Delta\nu$**1**)					
C_2H_4	3111	-	-	-	3095	3098	3093	**3**	-2
	2995	-	-	-	3001	3003	2998	**2**	-3
	1440	-	-	-	1420	1423	1423	**3**	3
	947	-	967	**- (20)**	940	961	937	**21**	-3
HNC	3620	3449	3467	**-171 (-153)**	3657	3492	3656	**-165**	-1
	2029	2028	2026	**-1 (-3)**	2022	2022	2027	**0**	5

Table 2: Experimental (isolated and photoproduced in Ar matrix) and theoretical (B3LYP/cc-pVTZ, scaled with a 0.97 factor) wavenumbers (cm^{-1}) of **C**$_1$ (C_2H_4:HCN) and **C'**$_1$ (C_2H_4:HNC) complexes

($\Delta\nu = \nu_{complex} - \nu_{monomer}$ with $\Delta\nu$dep for the C_2H_4/HCN/Ar experiment and $\Delta\nu$1 for 1 photolysis

Wavenumbers (cm^{-1}) and relative intensities of **6**	
Theory (B3LYP/cc-pVTZ)	Experimental
3338 (2)	-
3063 (1)	-
3012 (4)	-
2970 (6)	-
2929 (12)	-
2053 (100)	2043 (100)
1463 (1)	-
1441 (2)	-
1375 (1)	-
1367 (4)	-
1131 (2)	-
1057 (3)	-
1041 (34)	-
1025 (22)	-
867 (3)	-
860 (15)	857 (26)

Table 3: Experimental (in Ar matrix) and theoretical (B3LYP/cc-pVTZ, scaled with a 0.97 factor) wavenumbers (cm^{-1}) and relative intensities of the ketenimine **6**.

	Experimental			Calculation (B3LYP/cc-pVTZ)		
	Monomer	**C$_3$** complex	Δν	Monomer	**C$_3$** complex	Δν
H_2C=NH	3263[c]	3260	**-3**	3289	3287	**-2**
	3036[d]	-	-	2981	2977	**-4**
	2926[d]	-	-	2890	2892	**2**
	1641[d]	-	-	1645	1643	**-2**
	1453[d]	-	-	1433	1430	**-3**
	1348[d]			1318	1326	**8**
	1123[d]	-	-	1123	1138	**15**
	1063[d]		-	1057	1060	**3**
	1059[d]	1068	**9**	1033	1039	**6**
C_2H_2	-	-	-	3378	3374	**-4**
	3289	3298	**9**	3278	3275	**-3**
	1974	1969	**-5**	1989	1986	**-3**
	737	740	**4**	737	744	**7**
		-	-	737	740	**3**

Table 4: Experimental and theoretical (B3LYP/cc_pVTZ, scaled with a 0.97 factor) wavenumbers (cm^{-1}) of **C$_3$** (C_2H_4:H_2C=NH) complex.

Wavenumber (cm^{-1})				
CH_3CH_2NC **2**	H_2C=CHCN **3**	H_2C=CHNC **4**	HC_3N **5**	H_3C-CH=C=NH **6**
2151	2235	2125	3315	2042
	1413	1629	2269	857
	972	1116	2076	
	958	921	667	

Table 5: Experimental wavenumbers (cm^{-1}) of main photoproducts of **1** photolysis.

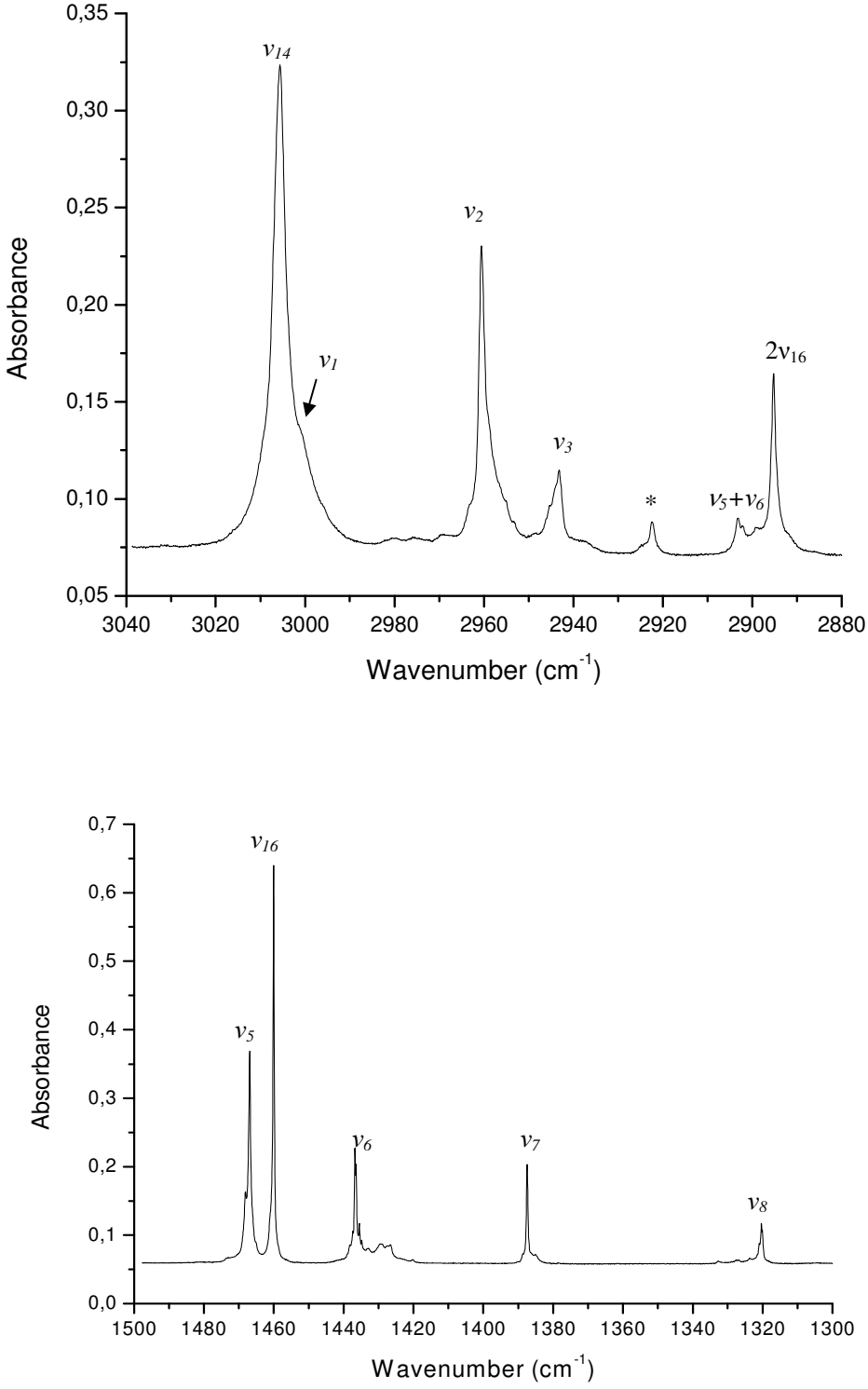

Figure 1: Different regions of the infrared spectrum at 20 K of **1** deposited in argon matrix (2/500). The band noted with an asterisk is attributed to an impurity.

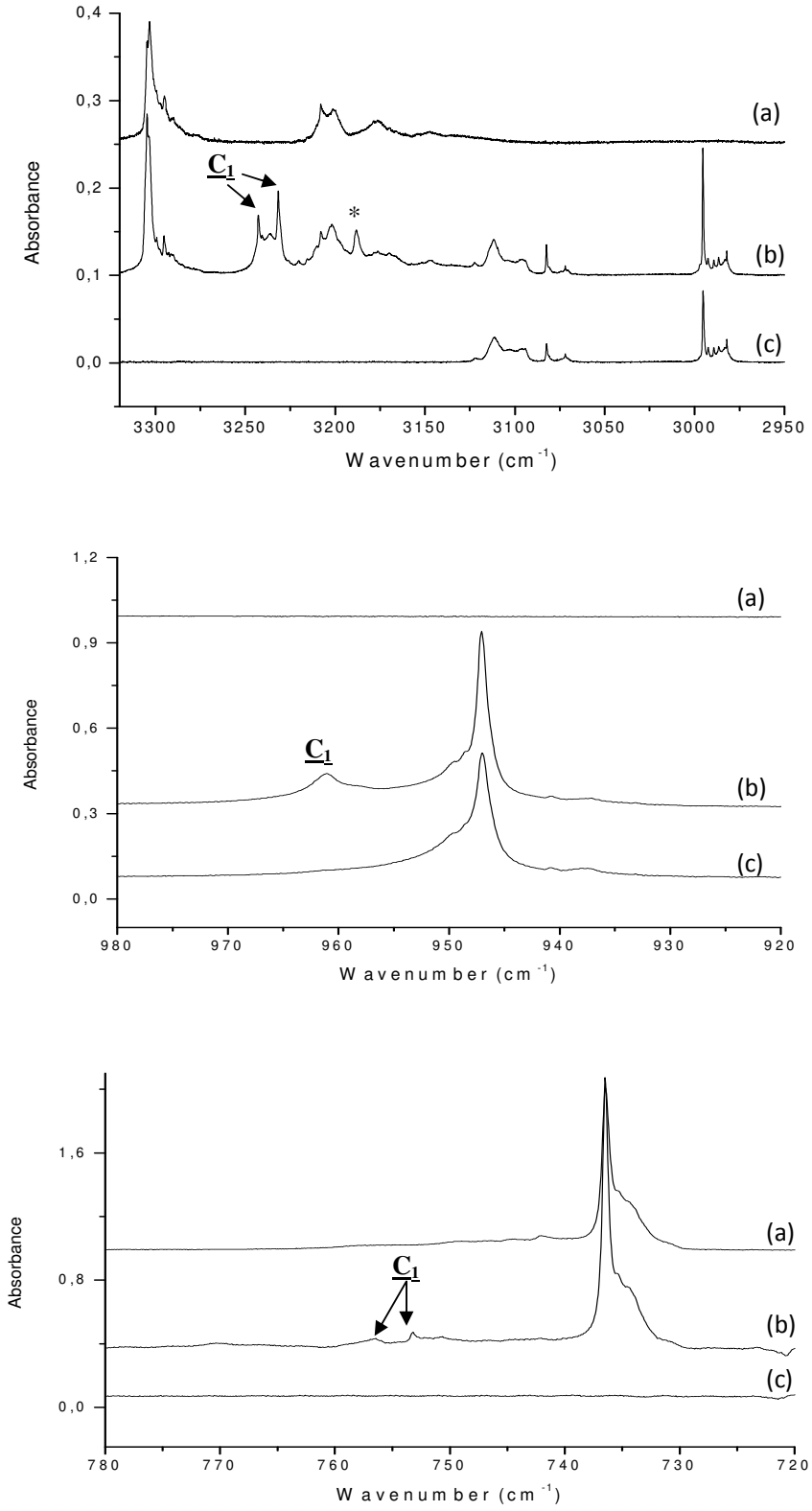

Figure 2: Infrared spectra for a 20 K deposition: (a) HCN/Ar 1/1000, (b) C_2H_4/HCN/Ar 1/5/1000, (c) C_2H_4/Ar 1/500. The band noted * remains unassigned.

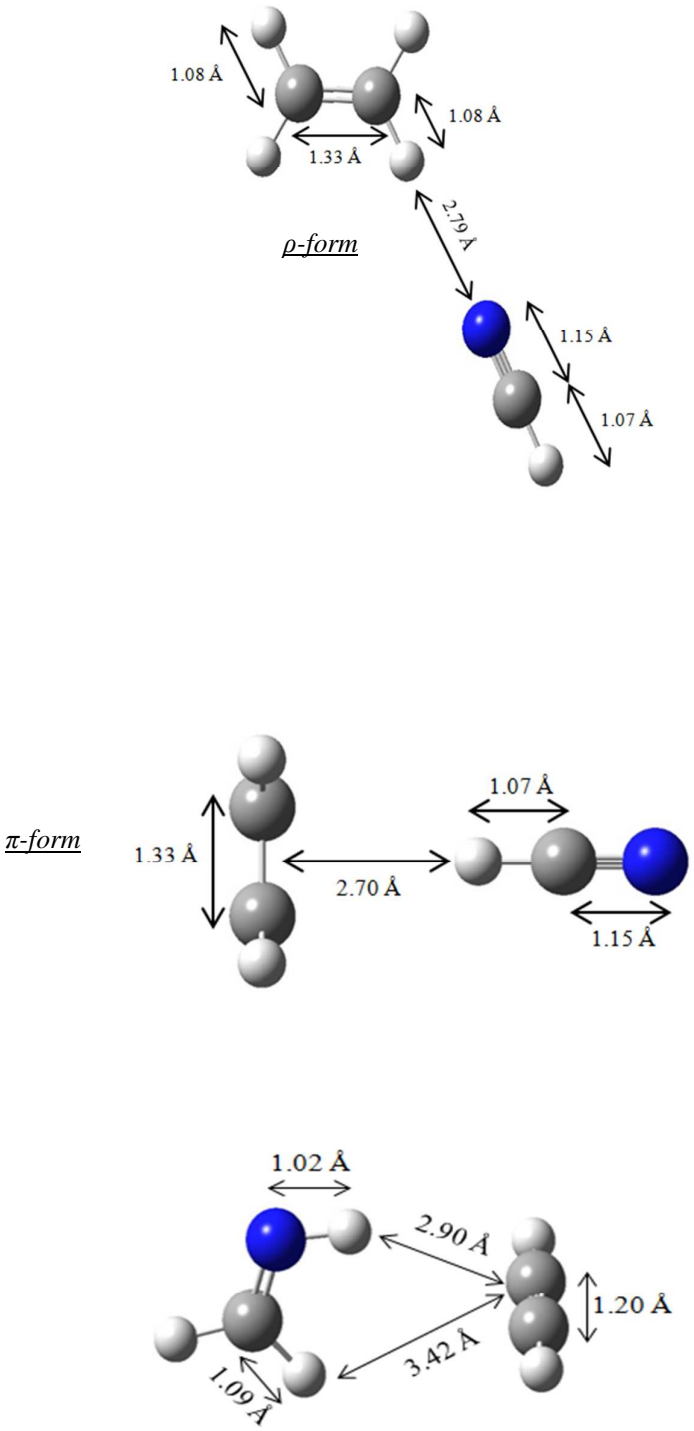

Figure 3: Optimized geometries (B3LYP/cc-pVTZ) of the ρ- and π-form C_1 complexes and of the C_3 complex (rCN = 1,26 Å).

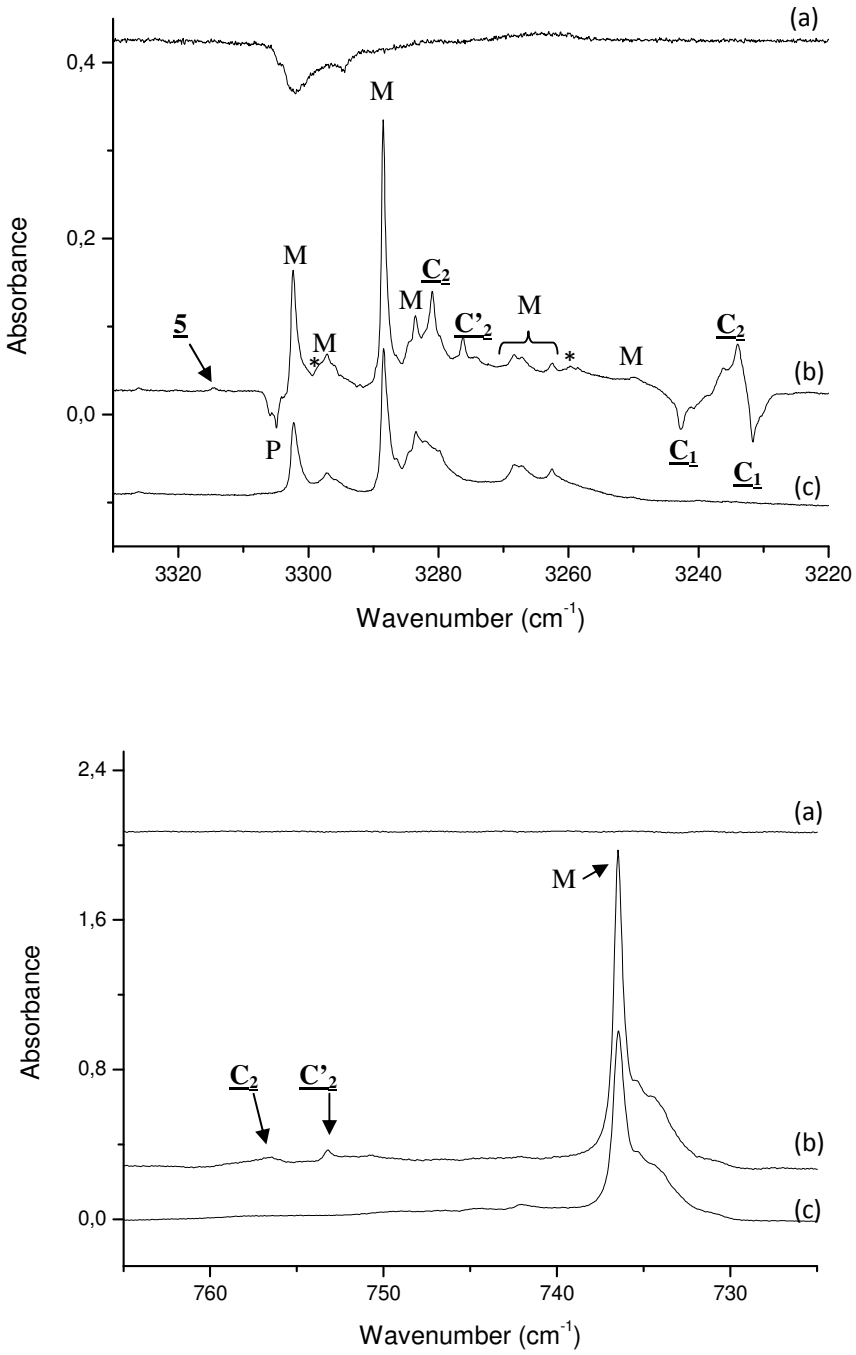

Figure 4: Subtraction infrared spectra after λ>120 nm photolysis : (a) HCN/Ar after 400 minutes (b) C_2H_4/HCN/Ar after 690 minutes and (c) C_2H_4/Ar after 390 minutes. The bands noted "M" corresponds to products coming from the photolysis of monomers. "P" corresponds to HCN polymers. The bands noted "*" remain unassigned.

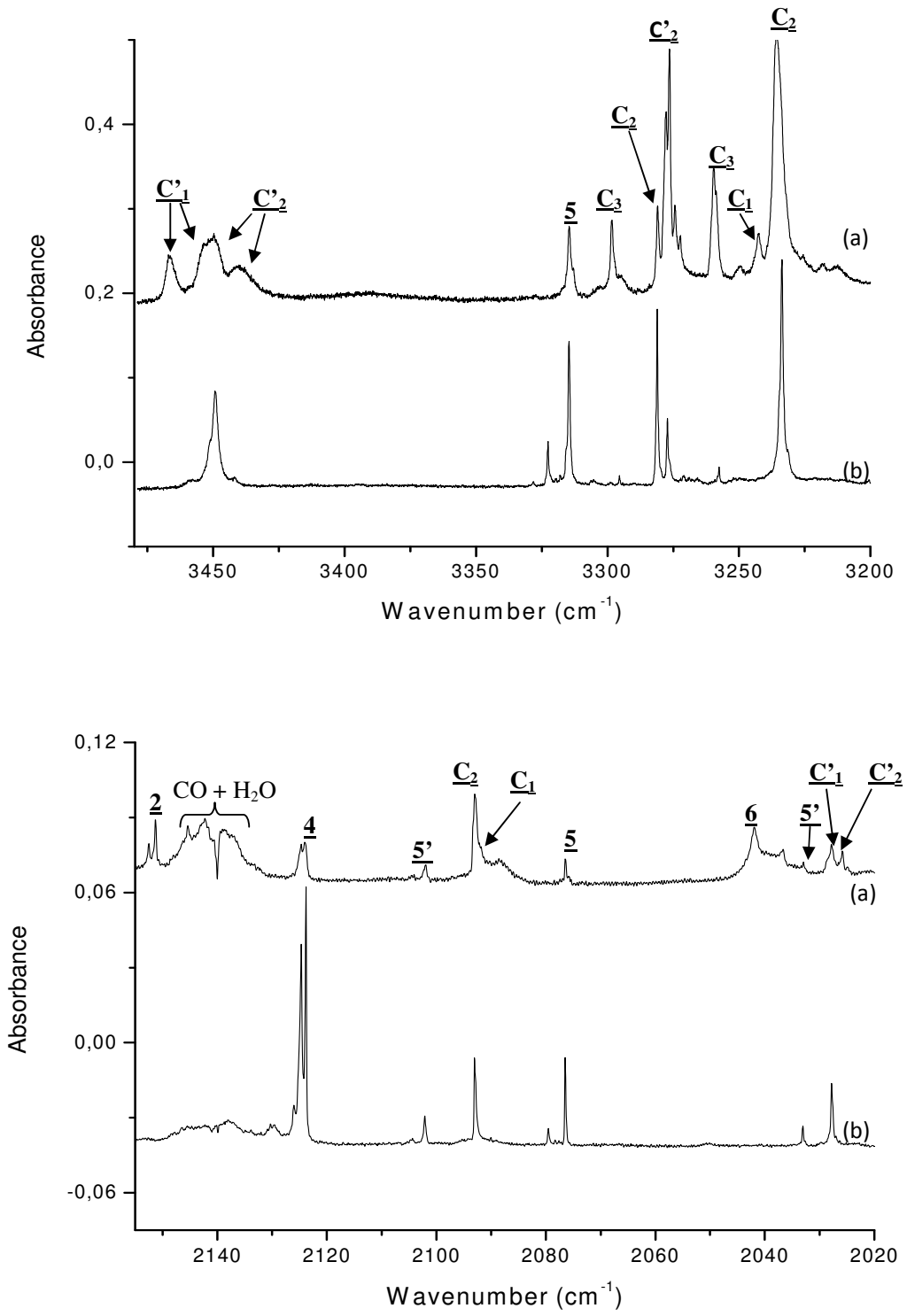

Figure 5: Infrared spectra of the λ>120 nm photolysis experiments of **1**: (a) subtraction spectrum after 1267 min of photolysis of **1**, (b) subtraction spectrum after 785 min of photolysis of **3**.

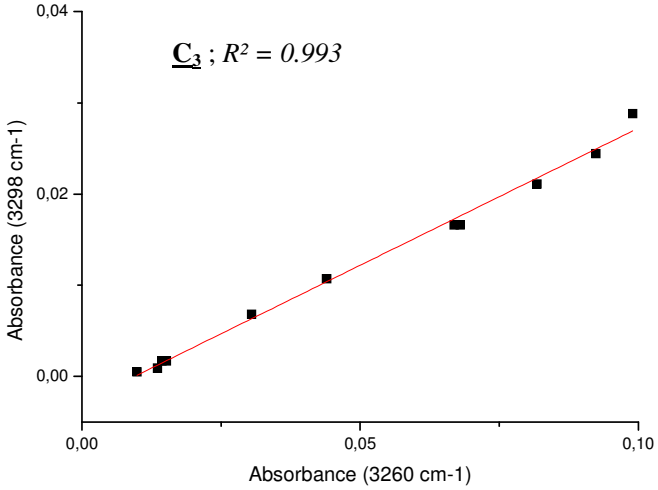

Figure 6: Cross-correlations of integrated optical densities for the most intense bands developed during far-UV irradiations of the **1**/Ar matrix, assigned to **C_3**

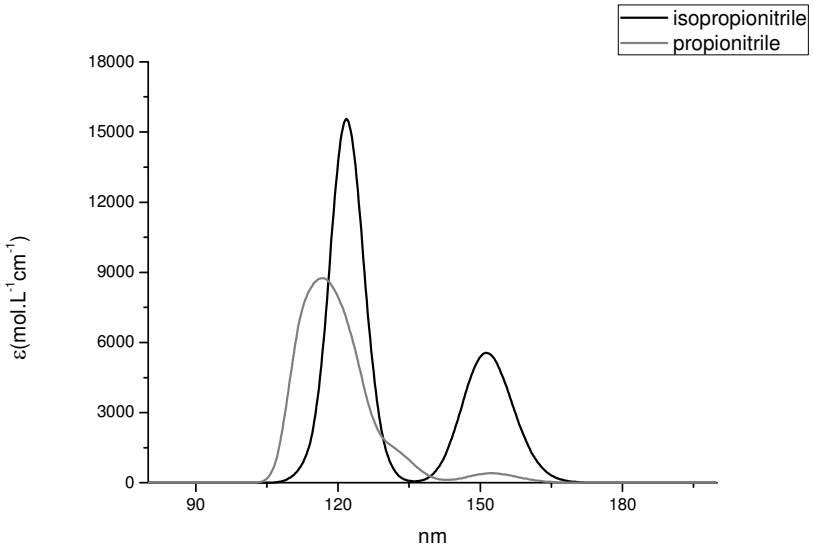

Figure 7: UV spectra of compounds **1** (grey line) and **2** (black line) in Argon calculated with TD-DFT

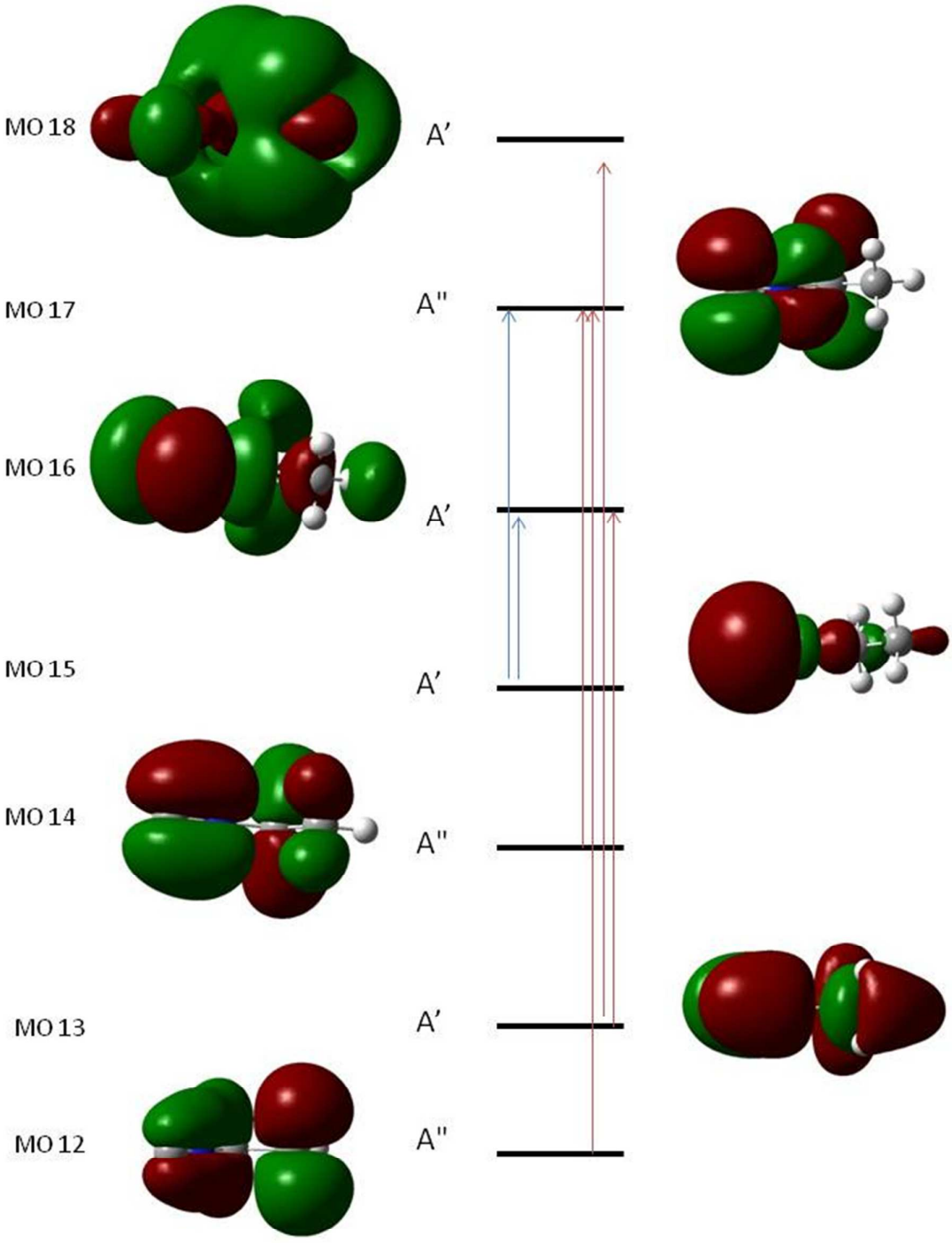

Figure 8: Representation of molecular orbitals (MOs) of **2** comprising $S_0 \rightarrow S_1$ for the absorption calculated at λ=122 and 151 nm

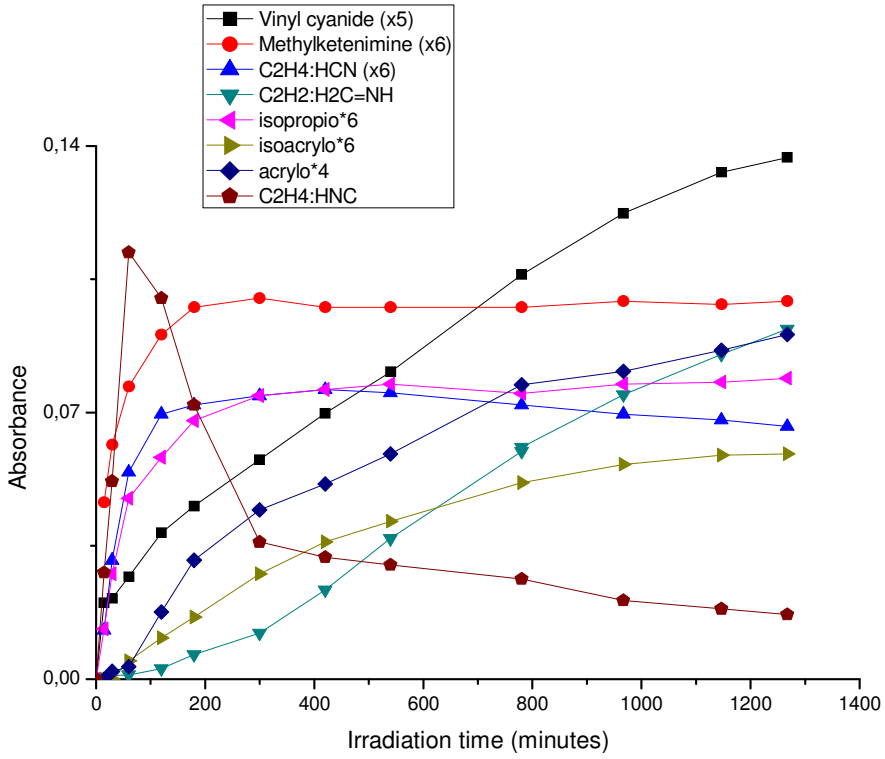

Figure 9: Evolution of the integrated absorbance of **2**, **3**, **4**, **6**, **C$_1$**, **C'$_1$** and **C$_3$** during λ>120 nm photolysis of **1**.

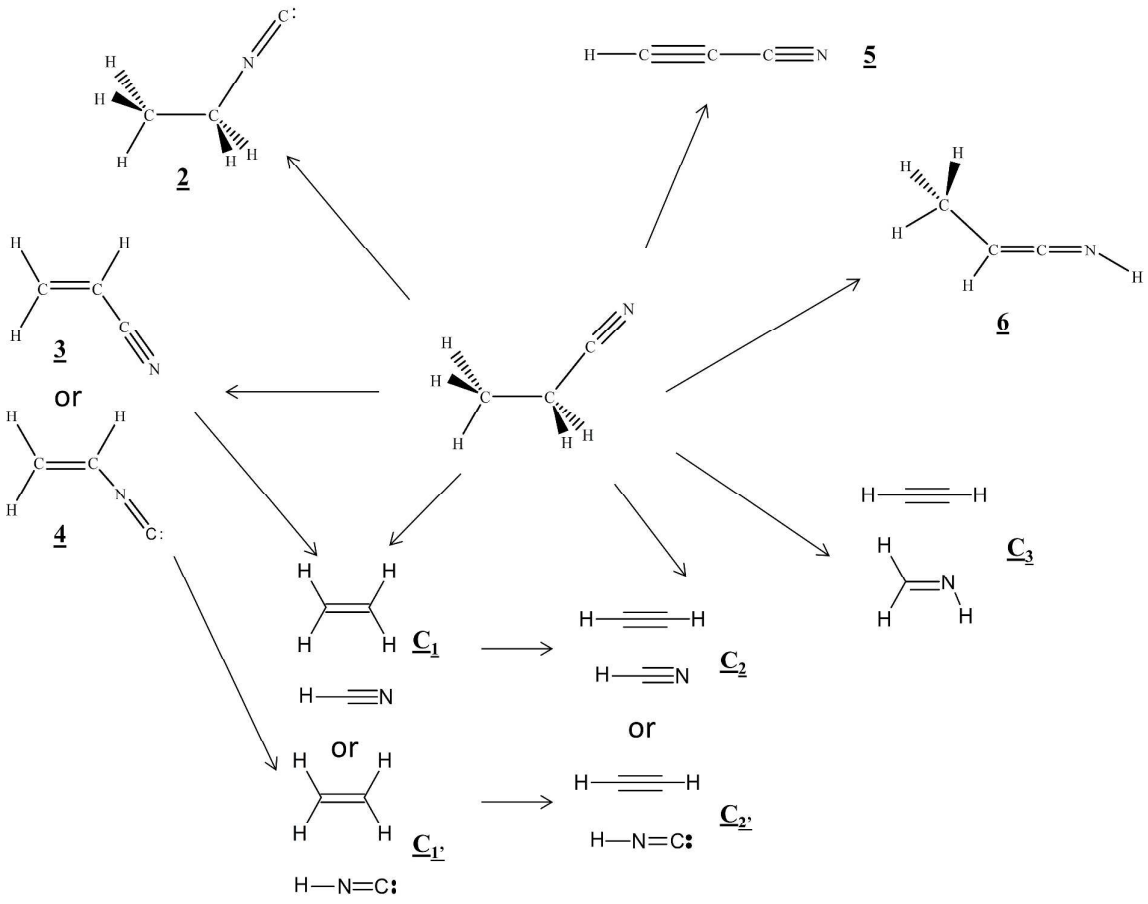

Scheme 1: Summary of the products formed after the photolysis of **1** (**2**: ethyl isocyanide; **3**: vinyl cyanide; **4**: vinyl isocyanide; **5**: cyanoacetylene; **6**: methylketenimine; $\mathbf{C_1}$, $\mathbf{C'_1}$, $\mathbf{C_2}$, $\mathbf{C'_2}$, $\mathbf{C_3}$: complexes).

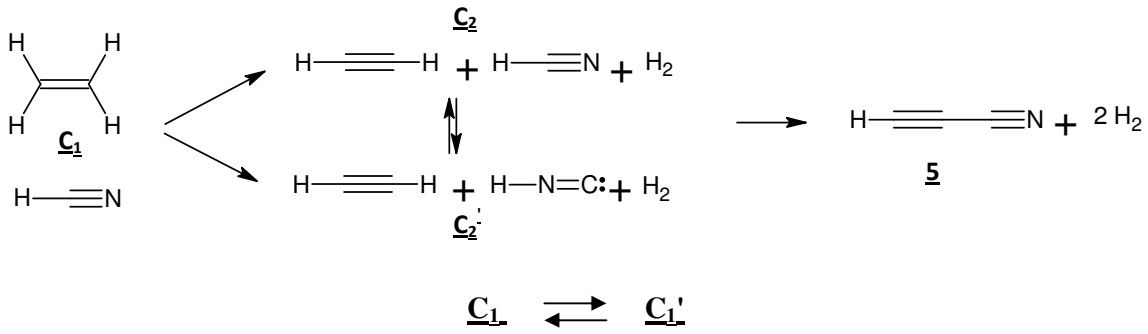

Scheme 2: Supposed reaction pathways for the photolysis products obtained by irradiation of C_2H_4:HCN complex (**C1**) at $\lambda > 120$ nm.

[1]A.L. Broadfoot, B.R. Sandel, D.E. Shemansky, J.B. Holberg, G.R. Smith, D.F. Strobel, J.C. McConnell, S. Kumar, D.M. Hunten, S.K. Atreya, T.M. Donahue, H.W. Moos, J.L. Bertaux, J.E. Blamont, R.B. Pomphrey, S. Linick; *Science*, 1981, **212**, 206.

[2] D.F. Strobel, D.E. Shemansky; *J. Geophys. Res. Spa. Phys.*, 1982, **87**, 1361.

[3] G.P. Kuiper; *Astrophys. J.*, 1944, **100**, 378.

[4] Y.L. Yung, M. Allen, J.P. Pinto; *Astrophys. J. Supp. Ser.*, 1984, **55**, 465.

[5] V.G. Kunde, A.C. Aikin, R.A. Hanel, D.E. Jennings, W.C. Maguire, R.E. Samuelson; *Nature*, 1981, **292**, 686.

[6] B. Letourneur, A. Coustenis; *Planet. Spa. Sci.*, 1993, **41**, 593.

[7] V. Vuitton, R.V. Yelle, V.G. Anicich; *Astrophys. J.*, 2006, **647**, 175.

[8] M.A. Cordiner, M.Y. Palmer, C.A. Nixon, P.G.J. Irwin, N.A. Teanby, S.B. Charnley, M.J. Mumma, Z. Kisiel, J. Serigano, Y.-J. Kuan, Y.-L. Chuang, K.-S. Wang; *Astrophys. J. Lett.*, 2015, in press.

[9] R.K. Khanna; *Icarus*, 2005, **177**, 116.

[10] D.R. Johnson, F.J. Lovas, C.A. Gottlieb, M.M. Litvak, M. Guélin, P. Thaddeus; *Astrophys. J.*, 1977, **218**, 370.

[11] V.A. Krasnopolsky; *Icarus*, 2009, **201**, 226.

[12] J.T. Herron; *J. Phys. Chem. Ref. Data*, 1999, **28**, 1453.

[13] N.E. Duncan, G.J. Janz; *J. Chem.Phys.*, 1954, **23**, 434.

[14] P. Klaboe, J. Grundnes; *Spectr. Acta A*, 1968, **24**, 1905.

[15] C.J. Wurrey, W.E. Bucy, J.R. Durig; *J. Phys.Chem.*, 1975, **80**, 1129.

[16] F. Cerceau, F. Raulin, R. Courtin, D. Gautier; *Icarus*, 1985, **62**, 207.

[17] G.A. Crowder; *Spectr. Acta A*, 1986, **42**, 1229.

[18] R.G. Lerner, B.P. Dailey; *J. Chem. Phys.*, 1957, **26**, 678.

[19] V.W. Laurie; *J. Chem. Phys.*, 1959, **31**, 1500.

[20] Y.S. Li, M.D. Harmony; *J. Chem. Phys.*, 1969, **50**, 3674.

[21] H. Mäder, U. Andresen, H. Dreizler; *Zeit. Naturfor.*, 1973, **28a**, 1163.

[22] H. Mäder, H.M. Heise, H. Dreizler; *Zeit. Naturfor.*, 1974, **29a**, 164.

[23] H.M. Heise, H. Lutz, H. Dreizler; *Zeit. Naturfor.*, 1974, **29a**, 1345.

[24] H.M. Heise, H. Mäder, H. Dreizler; *Zeit. Naturfor.*, 1976, **31a**, 1228.

[25] J. Burie, J. Demaison, A. Dubrulle, D. Boucher; *J. Mol. Spectrosc.*, 1978, **72**, 275.

[26] J.C. Pearson, K.V.L.N. Sastry, E. Herbst, F.C. De Lucia, *Astrophys. J. Suppl. Ser.*, 1994, **93**, 589.

[27] Y. Fukuyama, K. Omori, H. Odashima, K. Takagi, S. Tsunekawa; *J. Mol. Spectrosc.*, 1999, **193**, 72.

[28] N. Dello Russo, R.K. Khanna; *Icarus*, 2005, **123**, 366.

[29] J.A. Cutler; *J. Chem. Phys.*, 1948, **16**, 136.

[30] R.S. Stradling, A.G. Loudon; *J. Chem. Soc.*, *Fara. Trans. II*, 1977, **73**, 623.

[31] R.F. Lake, H. Thompson; *Proc. Roy. Soc. London A*, 1970, **317**, 187.

[32] K. Kanda, T. Nagata, T. Ibuki; *Chem. Phys.*, 1999, **243**, 89.

[33] R.L. Hudson, M.H. Moore; *Icarus*, 2004, **172**, 466.

[34] J. Pourcin, M. Monnier, P. Verlaque, G. Davidovics, R. Lauricella, C. Colonna, H. Bodot; *J. Mol. Spectrosc.*, 1985, **109**, 186.

[35] A. Toumi, N. Piétri, T. Chiavassa, I. Couturier-Tamburelli; *Icarus*, 2014, doi:http://dx.doi.org/10.016/j.icarus.

[36] M.S. Gudipati, R. Jacovi, I. Couturier-Tamburelli, A. Lignell, M. Allen; *Nature Communications 4*, 2013, **1648**, DOI: 10.1038/ncomms2649.

[37] I. Couturier-Tamburelli, M.S. Gudipati, A. Lignell, R. Jacovi, N. Piétri; *Icarus*, 2014, **234**, 81.

[38] P. Hohenberg, W. Kohn; *Phys. Rev. B*, 1964, **136**, 864.

[39] W. Kohn, L.J. Sham; *Phys. Rev. A*, 1965, **140**, 1133.

[40] W. Koch, M.C. Holthausen; *A Chemist's Guide to Density Functional Theory*, Wiley: Weinheim, Germany, 2002.

[41] M.J. Frisch, M.J. Trucks, H.B. Schlegel, G.E. Scuseria, M.A. Robb, J.R. Cheeseman, G. Scalmani, V. Barone, B. Menucci, G.A. Petersson, et al.; *Gaussian 09*, revision A02; Gaussian Inc.: Wallingford, CT, 2009.

[42] C. Lee, W. Yang, R.G. Parr; *Phys. Rev. B*, 1988, **37**, 785.

[43] A.D. Becke; *J. Chem. Phys.*, 1993, **98**, 5648.

[44] C. Lee, W. Yang, R.G. Parr, *Phys. Rev. B*, 1988, **37**, 785.

[45] A. Toumi, I. Couturier-Tamburelli, T. Chiavassa, N. Piétri; *J. Phys. Chem. A*, 2014, **118**, 2453.

[46] a- Z. Guennoun, I. Couturier-Tamburelli, S. Combes, J.P. Aycard, N. Piétri, *J. Phys. Chem. A*, 2005, **109**, 11733.
b- S. G. Kukolich, W. G. Read, P. D. Aldrich, *J. Chem. Phys.*, 1983, **78**, 3552.

[47] K. Bolton, N.L. Owen, J. Sheridan; *Spectr. Acta A*, 1969, **25**, 1.

[48] A. Coupeaud, M. Turowski, M. Gronowski, N. Piétri, I. Couturier-Tamburelli, R. Kołos, J.P. Aycard, *J. Chem. Phys.*, 2007, **126**, 164-301.

[49] Z. Guennoun, I. Couturier-Tamburelli, N. Piétri, J.P. Aycard; *Chem. Phys. Lett.*, 2003, **368**, 574.

[50] Z. Guennoun, A. Coupeaud, I. Couturier-Tamburelli, N. Piétri, S. Coussan, J.P. Aycard; *Chem. Phys.*, 2004, **300**, 143.

[51] R. Kołos, J. Waluk; *J. Mol. Struct.*, 1997, **408**, 473.

[52] R. Kołos, A.L. Sobolewski; *Chem. Phys. Lett.*, 2001, **344**, 625.

[53] R. Kołos, M. Gronowski, P. Botschwina; *J. Chem. Phys.*, 2008, **128**, 154305.

[54] Landolt-Börnstein, 1951, vol. 1, 6 ed., Springer, Berlin.

[55] D. Wang, X. Qian; *J. Elec. Spectrosc. Rel. Phen.*, 1997, **83**, 41.

[56] L.M. Yam, M.J. Shultz, E.J. Rok, S. Buchau, *J. Phys. Chem.*, 1988, **92**, 4632.

[57] W. Haag, J. Miale; MOBILE OIL CO, United States, patent number 3821278.

[58] G. Hunt, *New Scientist*, Nov. 1974, **64**, 429.

[59] M. Fulchignoni, A. Aboudan, F. Angrilli, M. Antonello, S. Bastianello, C. Bettanini, G. Bianchini, G. Colombatti, F. Ferri, E. Flamini, V. Gaborit, N. Ghafoor, B. Hathi, A.M. Harri, A. Lehto, P.F.L. Stoppato, M.L. Patel, J.C. Zarnecki; *Planet. Spa. Sci.*, 2004, **52**, 867.

[60] J. Cui, R.V. Yelle, V. Vuitton, J.H. Waite Jr, W.T. Kasprzak, D.A. Gell, H.B. Niemann, I.C.F. Müller-Wordarg, N. Borggren, G.G. Fletcher, E. Raaen, B.A. Magee; *Icarus*, 2009, **200**, 581.

[61] V.G. Kunde, A.C. Aikin, R.A. Hanel, D.E. Jennings, W.C. Maguire, R.E. Samuelson; *Nature*, 1981, **292**, 688.

[62] R.A. Hanel, B.J. Conrath, F.M. Flasar, V. Kunde, W. Maguire, J. Pearl, J. Pirraglia, R. Samuelson, L. Herath, M. Allison, D. Cruikshank, D. Gautier, P. Gierasch, L. Horn, L. Koppany, C. Ponnamperuma, *Science*, 1981, **212**, 192.

[63] R. Moreno, E. Lellouch, L.M. Lara, R. Courtin, D. Bockelée-Morvan, P. Hartogh, M. Rengel, N. Biver, M. Banaskiewicz, A. González, *Astron. Astrophys.*, 2011, **536**, 12.